

Coherent umklapp scattering of light from disordered photonic crystals

A. Yu. Sivachenko, M. E. Raikh, and Z. V. Vardeny

Department of Physics, University of Utah, Salt Lake City, Utah 84112

(Received 5 January 2001; published 14 May 2001)

A theoretical study of the coherent light scattering from disordered photonic crystals is presented. In addition to the conventional enhancement of the reflected light intensity into the backscattering direction, the so-called coherent backscattering (CBS), the periodic modulation of the dielectric function in photonic crystals gives rise to a qualitatively new effect: enhancement of the reflected light intensity in directions different from the backscattering direction. These additional coherent scattering processes, dubbed here *umklapp scattering* (CUS), result in peaks, which are most pronounced when the incident light beam enters the sample at an angle close to the the Bragg angle. Assuming that the dielectric function modulation is weak, we study the shape of the CUS peaks for different relative lengths of the modulation-induced Bragg attenuation compared to the disorder-induced mean free path. We show that when the Bragg length increases, then the CBS peak assumes its conventional shape, whereas the CUS peak rapidly diminishes in amplitude. We also study the suppression of the CUS peak upon the departure of the incident beam from the Bragg resonance: we found that the diminishing of the CUS intensity is accompanied by substantial broadening. In addition, the peak becomes asymmetric.

DOI: 10.1103/PhysRevB.63.245103

PACS number(s): 71.55.Jv, 42.70.Qs, 42.25.Dd

I. INTRODUCTION

Since the first experimental observations,¹⁻⁸ the phenomenon of coherent backscattering (CBS) of light from disordered media has been the subject of intense theoretical and experimental studies⁹ (see also Ref. 10 for the most recent review). The underlying mechanism for the CBS was identified as the interference of clockwise and counterclockwise scattering paths. This was understood already in the early works by analogy to the weak localization of electrons. It has been also pointed out¹¹ that this picture *fully* captures the physics of the coherent scattering only if there are no forbidden directions for the propagation of light in the absence of disorder. These forbidden directions emerge in systems with periodic spatial modulation of the dielectric function or, in other words, in photonic crystals with incomplete gaps.¹² In the presence of periodicity, the enhanced scattering of light may occur not only in the backscattering direction, but in other directions as well. Roughly speaking, the additional peaks in the scattering intensity can be regarded as periodicity-induced diffraction satellites of the CBS peak. Their origin is illustrated in Fig. 1. In the presence of the periodic modulation of the dielectric function, the light-wave vector is determined only up to the vector σ of the reciprocal lattice. Hence, upon entering the medium, light with wave vector k acquires a satellite component with y projection of the wave vector, $k_y = k \sin \theta - \sigma$. Importantly, the same argument also applies for the coherently backscattered light with wave vector $-k$, when it propagates inside the medium on the way out; namely, it also acquires a component with y projection $k_y = -k \sin \theta + \sigma$ (Fig. 1). This component gives rise to a satellite of the CBS peak in the direction θ' where $\sin \theta' = (\sigma - k \sin \theta)/k$. We dub this peak in the reflected light intensity as coherent *umklapp scattering* (CUS). We note that the above picture is only illustrative. In reality, in addition to the process shown in Fig. 1, a variety of diffraction processes contribute to the formation of the CUS peaks. In general, the

total number of the CUS peaks is determined by the number of reciprocal-lattice vectors for which $|-k + \sigma| < k$.

It follows from the above qualitative picture that the magnitude of the CUS peak is governed by the ratio of the disorder-induced mean free path l (the elementary step of light diffusion) and the characteristic length ξ of formation of the diffraction component. This formation occurs most efficiently for the incidence angles $\theta = \theta_B$, corresponding to the Bragg condition $k_y = \sigma/2$, i.e., $\sin \theta_B = \sigma/(2k)$. In this case ξ coincides with the Bragg decay length L_B , which is the decay length of the evanescent wave with frequency in the middle of the photonic stop band. Away from the Bragg resonance the length ξ increases, resulting in suppression of the CUS peak. We note that the limiting case $L_B \rightarrow 0$ and $\theta = \theta_B$ was considered in Ref. 13. In this case the CBS and CUS peaks are simply the mirror images of each other. In the case of a photonic crystal with an incomplete gap, L_B is large ($kL_B \gg 1$). The question of interest is then: how do the magnitude and shape of the CUS peak depend on L_B/l and on

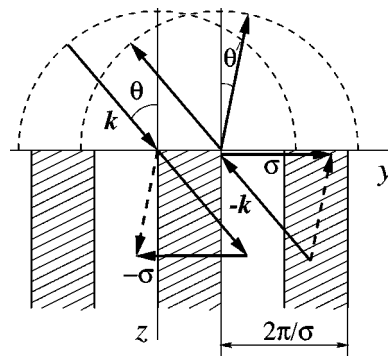


FIG. 1. Schematic plot of light diffraction in a photonic crystal. The diffraction satellites of the incident (at angle θ) and outgoing plane waves are shown with dashed lines. The diffraction satellite of the backscattered wave ($-k$) results in an outgoing wave emerging at an angle θ' .

the deviation of the incident beam from the Bragg angle? This question is studied in the present paper. We generalize the approach of Refs. 3 and 14 to the case of a periodically modulated dielectric medium and derive analytical expressions for the CBS and CUS peaks. We trace the evolution of the amplitude and width of the CUS peak with changing the parameter L_B/l and the incidence angle θ . We found that the most pronounced variation occurs within the domain $L_B \lesssim l$ and $(\theta - \theta_B) \lesssim (kL_B)^{-1}$.

The paper is organized as follows. In Sec. II we review the conventional derivation of the CBS and introduce the modifications necessary to take into account the Bragg reflection in periodic structure. In Sec. III we derive analytical expressions for the CUS and CBS albedo from a disordered photonic crystal and analyze limiting cases. In concluding remarks, Sec. IV, we outline a generalization of our theory for the case of arbitrary direction of the modulation wave vector.

II. COHERENT ALBEDO

A. Coherent backscattering from a disordered medium

In order to introduce the notations used throughout this paper, we first review the conventional derivation of the CBS following Ref. 14. Neglecting the polarization effects,¹⁵ the intensity $I(\mathbf{R})$, reflected from the medium when illuminated with incident flux F_0 and which is observed at point \mathbf{R} , is given by the well-known expression,¹⁴

$$I(\mathbf{R}) = F_0 \int G(\mathbf{R}, \mathbf{r}'_1) G^*(\mathbf{R}, \mathbf{r}'_2) U(\mathbf{r}_1, \mathbf{r}'_1, \mathbf{r}_2, \mathbf{r}'_2) \times \Psi_{inc}(\mathbf{r}_1) \Psi_{inc}^*(\mathbf{r}_2) \times d^3 r_1 d^3 r_2 d^3 r'_1 d^3 r'_2, \quad (1)$$

where $G(\mathbf{R}, \mathbf{r})$ is the mean propagator from \mathbf{r} (inside the medium) to the observation point \mathbf{R} , $\Psi_{inc}(\mathbf{r})$ is the normalized mean incident field at point \mathbf{r} inside the medium, and $U(\mathbf{r}_1, \mathbf{r}'_1, \mathbf{r}_2, \mathbf{r}'_2)$ is the sum of all scattering diagrams with the ends stripped.¹⁴

There are two leading contributions to $U(\mathbf{r}_1, \mathbf{r}'_1, \mathbf{r}_2, \mathbf{r}'_2)$. The first one comes from the ladder diagrams and describes the background incoherent scattering. The second contribution, which is responsible for the coherent enhancement of scattered intensity, represents the sum of maximally crossed diagrams

$$U_i(\mathbf{r}_1, \mathbf{r}'_1, \mathbf{r}_2, \mathbf{r}'_2) = \frac{4\pi c}{l^2} P(\mathbf{r}_1, \mathbf{r}'_1) \delta(\mathbf{r}_1 - \mathbf{r}'_2) \delta(\mathbf{r}'_1 - \mathbf{r}_2), \quad (2)$$

where $P(\mathbf{r}_1, \mathbf{r}'_1)$ is the stationary probability distribution to travel diffusively from \mathbf{r} to \mathbf{r}'_1 inside the scattering medium. For the disordered medium with a boundary, this probability distribution is given by

$$P(\mathbf{r}_1, \mathbf{r}'_1) = \frac{1}{4\pi D |\mathbf{r}_1 - \mathbf{r}'_1|} - \frac{1}{4\pi D |\mathbf{r}_1 - \mathbf{r}'_1^*|}, \quad (3)$$

where $D = lc/3$ is the light diffusion constant and c is the speed of light. The first term in Eq. (3) is a conventional propagator in the bulk medium. The second term ensures the boundary condition $P(z_0, \mathbf{r}'_1) = P(\mathbf{r}_1, z_0) = 0$ that is imposed to describe the diffusion inside a semi-infinite medium. The point \mathbf{r}'_1^* is the mirror image of the point \mathbf{r}'_1 with respect to the trapping plane located at $z_0 \approx -0.7l$ (see Ref. 10 and references therein).

The mean incident field in the case of a translationally invariant (on average) system is given by

$$\Psi_{inc}(\mathbf{r}_1) = \exp\left(-\frac{z_1}{l \cos \theta} + i\mathbf{k}\mathbf{r}_1\right), \quad (4)$$

where \mathbf{k} is the wave vector of the incident light ($|\mathbf{k}| = k = \omega/c$) and θ is the angle of incidence (Fig. 1). The first term in the exponent describes the decay of the incident mean-field amplitude due to scattering.

For the observation point \mathbf{R} in the far-field region, the asymptotic expansion of the Green's function $G(\mathbf{R}, \mathbf{r}_1)$ is

$$G(\mathbf{R}, \mathbf{r}_1) \approx \frac{e^{ikR}}{4\pi R} \exp\left(-\frac{z_1}{l \cos \theta'} - i\mathbf{k}'\mathbf{r}_1\right), \quad (5)$$

where \mathbf{k}' is the wave vector in the direction of observation, $|\mathbf{k}'| = \omega/c$, and θ' is the angle between \mathbf{k} and the z axis.

Substitution of Eqs. (2)–(5) into Eq. (1) results in the following expression for the CBS albedo α , defined as the scattered intensity divided by the incident flux and the sample area S ,

$$\alpha(\mathbf{k}, \mathbf{k}') = \frac{3}{(4\pi)^2 S l^3} \int d^2 \boldsymbol{\rho} dz_1 dz'_1 \times \exp\left[i\mathbf{q}\boldsymbol{\rho} + i\kappa(z_1 - z'_1) - b \frac{(z_1 + z'_1)}{l}\right] \times \left(\frac{1}{\sqrt{\rho^2 + (z_1 - z'_1)^2}} - \frac{1}{\sqrt{\rho^2 + (z_1 + z'_1 + 2z_0)^2}}\right), \quad (6)$$

where $\boldsymbol{\rho}$ is the component of $(\mathbf{r}_1 - \mathbf{r}'_1)$ parallel to the medium boundary, $\kappa = (\mathbf{k} + \mathbf{k}')_z$, $\mathbf{q} = \{(\mathbf{k} + \mathbf{k}')_x, (\mathbf{k} + \mathbf{k}')_y\}$, and $b = (1/\cos \theta + 1/\cos \theta')$. Due to the presence of the fast oscillating exponent, $\exp(i\mathbf{q}\boldsymbol{\rho})$, the integral in Eq. (6) is nonzero only within a narrow interval $|\theta' - \theta| \sim (kl)^{-1}$ around the backscattering direction, i.e., $\mathbf{q} = 0$. In Ref. 14 this integral was evaluated analytically for small angles θ, θ' . In fact, a general expression that is valid for arbitrary θ, θ' can be obtained,

$$\alpha(\mathbf{k}, \mathbf{k}') = f(\kappa, \mathbf{q}, b) = \frac{3}{8\pi S} \frac{1}{(\kappa l)^2 + (b + ql)^2} \times \left[\frac{1}{b} + \frac{1 - \exp(-2qz_0)}{ql}\right]. \quad (7)$$

In Sec. II B we trace how the albedo (7) is modified in the presence of a weak periodic modulation of the dielectric function inside the scattering medium.

B. Coherent scattering in the presence of a photonic crystal

1. Modification of the wave amplitudes

Our main observation is that an incomplete photonic gap affects light diffusion only weakly.¹⁶ The probability that a certain step of the diffusive motion occurs in the forbidden direction can be estimated as $(kL_B)^{-1} \ll 1$. On the other hand, *before the first* and *after the last* scattering events the light propagates along fixed directions θ and θ' . If either θ or θ' is close to the forbidden direction, then light propagation will be strongly affected, resulting in a significant change in the albedo. This observation suggests that in order to calculate the coherent albedo from a photonic crystal with an incomplete gap, it is sufficient to modify only the incident field amplitude in Eq. (4) and the Green function of emerging light in Eq. (5), without changing the propagator in Eq. (2).

To model the incomplete band gap, which is narrow compared to the Bragg frequency, one can keep only a single harmonics in the spatial modulation of the dielectric function,

$$\delta\varepsilon(y) = 2\delta\varepsilon \cos(\sigma y). \quad (8)$$

Here we assumed for simplicity that the direction of modulation is parallel to the boundary as shown in Fig. 1. Generalization of the results to an arbitrary angle between the boundary and the modulation wave vector is outlined in the concluding remarks.

As was pointed out above, the Bragg resonance condition has the form $k_y = \sigma/2$. For a wave propagating in a boundless medium this condition would lead to an amplitude decay $\propto \exp[-\text{Im}(k_y)y]$ in the y direction, for light within the frequency range $\Delta\omega \approx \sigma c \delta\varepsilon$ (the photonic stop band). However, the boundary conditions enforce a real k_y value (see Fig. 1). Consequently, instead of causing a finite $\text{Im}(k_y)$, the Bragg condition manifests itself in splitting of the z projection of the wave vector. This may be seen from the following relation between the components of the wave vector $\tilde{\mathbf{k}}$ inside the medium in the vicinity of the Bragg resonance,

$$\cos^2 \theta_B (\delta\tilde{k}_z)^2 - \sin^2 \theta_B (\delta\tilde{k}_y)^2 = \left(\frac{k \delta\varepsilon}{2} \right)^2, \quad (9)$$

where $\delta\tilde{k}_z = \tilde{k}_z - k \cos \theta_B$ and $\delta\tilde{k}_y = \tilde{k}_y - k \sin \theta_B$. The derivation of Eq. (9) is sketched in the Appendix. With $\tilde{k}_y = k_y = k \sin \theta$ fixed by the boundary conditions, Eq. (9) yields two values of \tilde{k}_z , namely $\tilde{k}_z = k \cos \theta_B \pm \Omega$ with

$$\begin{aligned} \Omega &= \frac{1}{2k \cos \theta_B} \sqrt{(\sigma k \cos \theta_B \beta)^2 + (k^2 \delta\varepsilon)^2} \\ &= \frac{\tan \theta_B}{2L_B} \sqrt{(2kL_B \cos \theta_B \beta)^2 + 1}, \end{aligned} \quad (10)$$

where $\beta = \theta - \theta_B$ is the deviation from the Bragg angle and $L_B = 2 \sin^2 \theta_B / (\sigma \delta\varepsilon)$ is the Bragg length. In the region $z > 0$, the field components with z projections $k \cos \theta_B + \Omega$ and $k \cos \theta_B - \Omega$, which comprise the waves $\tilde{\mathbf{k}}$ and $\tilde{\mathbf{k}} - \boldsymbol{\sigma}$ shown in Fig. 1, are coupled to each other. This leads to the following modification of Eq. (4) for Ψ_{inc} :

$$\begin{aligned} \Psi_{inc}(\mathbf{r}) &\approx \exp\left(-\frac{z}{l \cos \theta_B}\right) \\ &\times \{C_{\Omega, \phi}(z) e^{i\mathbf{k}_B \mathbf{r}} + iS_{\Omega, \phi}(z) e^{i(\mathbf{k}_B - \boldsymbol{\sigma}) \mathbf{r}}\}, \end{aligned} \quad (11)$$

where the functions $C_{\Omega, \phi}(z)$ and $S_{\Omega, \phi}(z)$ are defined as

$$C_{\Omega, \phi}(z) = \cos(\Omega z) - i \cos \phi \sin(\Omega z), \quad (12)$$

$$S_{\Omega, \phi}(z) = \sin \phi \sin(\Omega z), \quad (13)$$

and ϕ is determined by the relation

$$\sin \phi = \frac{1}{\sqrt{(2kL_B \cos \theta_B \beta)^2 + 1}}. \quad (14)$$

The first term of the field amplitude in Eq. (11) is the wave transmitted through the interface and traveling along a direction close to the direction \mathbf{k} of the incident wave, $(\mathbf{k}_B)_z = k \cos \theta_B$ and $(\mathbf{k}_B)_{xy} = k_{xy} = k \sin \theta$. The second term is the diffracted satellite wave. As is seen in Eq. (13), the characteristic length scale at which the latter wave is formed is $\xi = 1/\Omega$. In the limit $L_B \rightarrow \infty$ the incident wave does not change upon crossing the boundary. Indeed, the satellite wave in Eq. (11) vanishes due to the $\sin \phi$ prefactor in Eq. (13), whereas $C_{\Omega, \phi}(z)$ turns into $\exp(-ik \sin \theta_B \beta z)$ and makes up for the difference between $(\mathbf{k}_B)_z$ and $k_z = k \cos \theta$.

The modification due to the Bragg scattering should be incorporated into the emerging wave propagator G in a similar way. Taking into account that after the last scattering event a wave $\exp(i\mathbf{k}' \mathbf{r})$ that emerges at angle $\theta' = \theta_B + \delta\theta$ close to the Bragg resonance also has a diffracted component inside the medium, Eq. (5) transforms into

$$\begin{aligned} G(\mathbf{R}, \mathbf{r}) &\approx \frac{e^{i\mathbf{k}' \mathbf{r}}}{4\pi R} \exp\left(-\frac{z}{l \cos \theta'}\right) \\ &\times \{C_{\Omega', \phi'}(z) e^{-i(\mathbf{k}'_B - \boldsymbol{\sigma}) \mathbf{r}} + iS_{\Omega', \phi'}(z) e^{-i\mathbf{k}'_B \mathbf{r}}\}, \end{aligned} \quad (15)$$

where Ω' and ϕ' are given by the same expressions (10) and (14), where β is replaced by $\delta\theta$. The components of the wave vector \mathbf{k}'_B inside the medium are given by $(\mathbf{k}'_B)_z = -k \cos \theta_B$ and $(\mathbf{k}'_B)_{xy} = k'_{xy} = k \sin \theta'$. Expression (15) is written specifically for the observation point in the CUS direction, i.e., $(\mathbf{k}_B)_y > 0$ (Fig. 1). Similarly to Eq. (11), $G(\mathbf{R}, \mathbf{r})$ represents the sum of two terms, which we dub here as the C term and S term, respectively.

2. CUS and CBS albedo

Substitution of Eqs. (11) and (15) together with Eqs. (2) and (3) into Eq. (1) produces a sum of various terms with fast oscillating exponential factors. The terms with factors

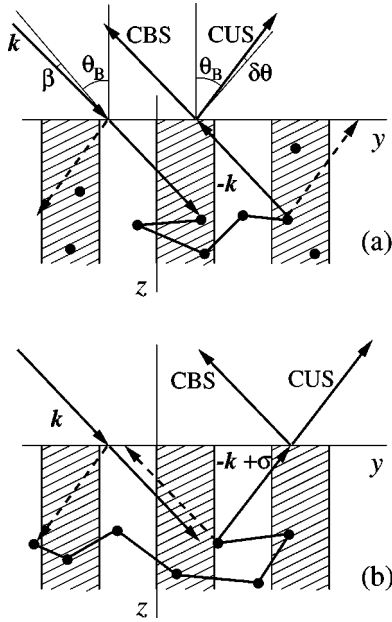


FIG. 2. Schematic illustration of different contributions to the coherent albedo. The CUS peak originates from (a) the diffraction of the backscattered light and (b) backscattering of the diffracted light.

$e^{\pm i\sigma r_1}$ or $e^{\pm i\sigma r'_1}$ average out upon integration. Since Eq. (15) is valid only in the vicinity of the Bragg resonance $\mathbf{k}' \approx -\mathbf{k} + \boldsymbol{\sigma}$, then nonresonant terms should be discarded. Note, however, that, in addition to the oscillating terms, the product of field amplitudes (11) and propagators (15) in Eq. (1) contains now *two* terms proportional to $\exp[i(\mathbf{k}'_B + \mathbf{k}_B - \boldsymbol{\sigma})\boldsymbol{\rho}]$, which *do not vanish* if the outgoing light is parallel to the CUS direction. The total CUS albedo is determined by these terms and is thus given by

$$\begin{aligned} \alpha_{CUS}(\mathbf{k}, \mathbf{k}') = & \frac{c}{4\pi l^2 S} \int d^2 \boldsymbol{\rho} dz_1 dz'_1 \\ & \times \exp\left[i\mathbf{q}\boldsymbol{\rho} - b \frac{(z_1 + z'_1)}{l}\right] P(\mathbf{r}_1, \mathbf{r}'_1) \\ & \times [C_{\Omega', \phi'}^*(z'_1) C_{\Omega, \phi}^*(z_1) S_{\Omega, \phi}(z_1) S_{\Omega', \phi'}^*(z_1) \\ & + C_{\Omega, \phi}(z_1) C_{\Omega', \phi'}^*(z_1) S_{\Omega', \phi'}(z'_1) S_{\Omega, \phi}^*(z'_1)], \end{aligned} \quad (16)$$

where $\mathbf{q} = (\mathbf{k}_B + \mathbf{k}'_B - \boldsymbol{\sigma})_{xy}$.

The origin of the two terms in the coherent scattering albedo is schematically illustrated in Fig. 2. In Fig. 2(a) the C component of the incident light (solid line) *first* experiences coherent backscattering and *then* is diffracted into the S component (dashed line). In Fig. 2(b) the C component of the incident light is *first* diffracted into the S component, the backscattering of which provides the second contribution to the CUS.

The origins of the *two* contributions to the CBS can be traced from Eq. (1) in a similar way (see also Fig. 2). The only technical difference between the derivations of the CBS

and CUS is that for the observation point \mathbf{R} in the CBS direction (i.e., $\mathbf{k}' \approx -\mathbf{k}$), $\boldsymbol{\sigma}$ should be added to the wave vectors in both oscillating exponents of the Green function in Eq. (15).

Substitution of the modified propagator into Eq. (1) and the selection of nonvanishing resonant terms produce the following expression for the CBS albedo:

$$\begin{aligned} \alpha_{CBS}(\mathbf{k}, \mathbf{k}') = & \frac{c}{4\pi l^2 S} \int d^2 \boldsymbol{\rho} dz_1 dz'_1 \\ & \times \exp\left[i\mathbf{q}\boldsymbol{\rho} - b \frac{(z_1 + z'_1)}{l}\right] P(\mathbf{r}_1, \mathbf{r}'_1) \\ & \times [C_{\Omega', \phi'}^*(z_1) C_{\Omega', \phi'}(z'_1) C_{\Omega, \phi}(z_1) C_{\Omega, \phi}^*(z'_1) \\ & + S_{\Omega', \phi'}^*(z_1) S_{\Omega', \phi'}(z'_1) S_{\Omega, \phi}(z_1) S_{\Omega, \phi}^*(z'_1)], \end{aligned} \quad (17)$$

with $\mathbf{q} = (\mathbf{k}_B + \mathbf{k}'_B)_{xy}$. In the limit $L_B \rightarrow \infty$, the diffracted waves vanish, $S_{\Omega, \phi} \rightarrow 0$, so that the only contribution to the albedo that survives in this limit comes from the first term of Eq. (17).

III. RESULTS AND DISCUSSION

A. Analytical results

1. Expressions for CBS and CUS albedo

The additional oscillating factors $C(z)$ and $S(z)$ in the integrands (16) and (17) compared to Eq. (6) can be formally absorbed into the decrement b by adding to it imaginary parts of the type $i(\Omega \pm \Omega')l$. Then all the contributions to the coherent albedo can be conveniently expressed with the help of an auxiliary function, $\tilde{f}(\kappa, p)$, defined as

$$\begin{aligned} \tilde{f}(\kappa, p) = & f(\kappa, q, b + ipl) + f(\kappa, q, b - ipl) \\ = & \frac{3}{4\pi SD} \frac{1}{1 + X^2} \left[\frac{b - p l X}{b^2 + p^2 l^2} + \frac{1 - e^{-2qz_0}}{ql} \right], \end{aligned} \quad (18)$$

where $f(\kappa, q, b)$ is the shape of the CBS cone given by Eq. (7); the parameters D and X are expressed through the arguments of the function f as follows:

$$D = (\kappa^2 - p^2)l^2 + (b + ql)^2, \quad (19)$$

$$X = \frac{2pl(b + ql)}{D}. \quad (20)$$

In Eq. (18) the wave vector q is equal to $q = k \cos \theta_B |\beta - \delta\theta|$ for the CBS, and $q = k \cos \theta_B |\beta + \delta\theta|$ for the CUS; in the vicinity of the Bragg resonance we can set $b = (\cos \theta)^{-1} + (\cos \theta')^{-1} \approx 2(\cos \theta_B)^{-1}$. Finally, the two contributions to the CBS albedo in Eq. (17) take the form

$$\begin{aligned}
\alpha_{CBS}^{(1)} = & \frac{\sin^2 \phi \sin^2 \phi'}{16} [\tilde{f}(0, \Omega + \Omega') + \tilde{f}(0, \Omega - \Omega')] \\
& + \frac{(1 + \cos^2 \phi)(1 + \cos^2 \phi')}{16} [\tilde{f}(\Omega + \Omega', 0) \\
& + \tilde{f}(\Omega - \Omega', 0)] + \frac{(1 + \cos^2 \phi) \sin^2 \phi'}{8} \tilde{f}(\Omega, \Omega') \\
& + \frac{(1 + \cos^2 \phi') \sin^2 \phi}{8} \tilde{f}(\Omega', \Omega) - \frac{\cos \phi \cos \phi'}{4} \\
& \times [\tilde{f}(\Omega + \Omega', 0) - \tilde{f}(\Omega - \Omega', 0)], \quad (21)
\end{aligned}$$

$$\begin{aligned}
\alpha_{CBS}^{(2)} = & \frac{\sin^2 \phi \sin^2 \phi'}{16} [\tilde{f}(\Omega + \Omega', 0) + \tilde{f}(\Omega - \Omega', 0) \\
& + \tilde{f}(0, \Omega + \Omega') + \tilde{f}(0, \Omega - \Omega') - \tilde{f}(\Omega', \Omega) \\
& - \tilde{f}(\Omega, \Omega')]. \quad (22)
\end{aligned}$$

Analogously, the CUS albedo Eq. (16) can be expressed through the function \tilde{f} in the following way:

$$\begin{aligned}
\alpha_{CUS} = & \frac{\sin \phi \sin \phi'}{8} \{ (1 + \cos \phi \cos \phi') [\tilde{f}(0, \Omega - \Omega') \\
& + \tilde{f}(\Omega - \Omega', 0) - \tilde{f}(\Omega, \Omega') - \tilde{f}(\Omega', \Omega)] \\
& - (1 - \cos \phi \cos \phi') [\tilde{f}(0, \Omega + \Omega') + \tilde{f}(\Omega + \Omega', 0) \\
& - \tilde{f}(\Omega, \Omega') - \tilde{f}(\Omega', \Omega)] \}. \quad (23)
\end{aligned}$$

Expressions (21)–(23) are our main results. Below we analyze two limiting cases of small and large L_B .

2. Limiting cases

Let us trace how the conventional CBS cone is recovered in the limit $L_B \rightarrow \infty$. In this limit we have $\phi, \phi' \rightarrow 0$, so that α_{CUS} and $\alpha_{CBS}^{(2)}$ containing $\sin \phi$ and/or $\sin \phi'$ as prefactors, vanish. Substituting $\phi = \phi' = 0$ into Eq. (21) we obtain $\alpha_{CBS}^{(1)} = f(\Omega - \Omega', q, b)$. Taking the limit $L_B \rightarrow \infty$ in Eq. (10), we get $(\Omega - \Omega') \rightarrow k \sin \theta_B (\beta - \delta \theta)$. Correspondingly, $f(\Omega - \Omega', q, b)$ reduces to Eq. (7).

Consider now the opposite limit,¹³ $L_B/l \ll 1$. In this limit $\phi, \phi' \rightarrow \pi/2$. It follows from Eq. (10) that with decreasing L_B both Ω and Ω' diverge, while $(\Omega - \Omega') \rightarrow 0$. As a result, as can be also seen from Eq. (18), all of the terms in Eqs. (21)–(23) that contain Ω , Ω' or $\Omega + \Omega'$ as at least one of the arguments, vanish. Then it is straightforward to check that both α_{CBS} and α_{CUS} take the form $\tilde{f}(0,0)/4 = f(0, q, b)/2$. We thus recover the result of Ref. 13 that in the limit of strong modulation, CBS and CUS cones are the mirror images of each other. Concerning the shape of the cones, it is given by the conventional expression (7) for the coherent albedo. Concerning the peak heights, they are two times less than the height of the CBS peak in the absence of modulation.

B. Shapes of the CBS and CUS peaks

Expressions (21)–(23) for the CBS and CUS albedo are valid only in the vicinity of the Bragg resonance $\theta, \theta' \approx \theta_B$. Note, however, that only in this region CUS has an appreciable amplitude. To illustrate this we plot in Fig. 3 the CBS and CUS cones for different detunings, $\beta = \theta - \theta_B$, of the incident beam from the Bragg angle for $L_B/l = 0.3$. It is seen that CUS practically dies out at $\beta \approx (2kL_B \cos \theta_B)^{-1} \ll 1$. It is also seen that as the amplitude of the CUS peak falls off, the peak also becomes asymmetric. The behavior of the CUS and CBS peak heights with the detuning β is summarized in Fig. 4.

Consider now the case of exact resonance, $\beta = 0$. As was discussed above, the relation between the CBS and CUS peaks is governed by the dimensionless parameter L_B/l . In Fig. 5 we show the heights of both peaks as functions of L_B/l . It is seen that the amplitude of the CBS peak saturates already at $L_B/l \gtrsim 2$; at the same time, the CUS peak diminishes by an order of magnitude.

In Fig. 6 we illustrate the evolution of the CUS cone at $\beta = 0$ with increasing L_B/l . For reference the CBS cone for $L_B/l = 0.3$ is also plotted in Fig. 6 (solid line). We note that while the CUS peak keeps narrowing for $L_B \leq l$, the shape of the CBS cone remains practically unchanged with L_B/l .

IV. CONCLUSIONS

In this paper we have studied coherent light scattering from a disordered photonic crystal with incomplete band gaps. We have demonstrated that the crystal dielectric function periodicity gives rise to additional coherent albedo peaks in nonbackscattering directions. These peaks emerge as the angle of incidence θ approaches the Bragg resonance, $\theta \approx \theta_B$. For simplicity, the consideration was restricted to the case where the modulation wave vector σ is parallel to the crystal boundary. In this case, and under the Bragg resonance condition $2k \sin \theta_B = \sigma$, the direction of the additional (CUS) peak coincides with the reflection direction, since the CUS wave vector is equal to $\mathbf{k}' = -\mathbf{k} + \sigma$. The component of \mathbf{k}' parallel to the boundary is equal to $k'_y = -k \sin \theta + \sigma$. Then at $\theta = \theta_B$ we have $k'_y = k_y = \sigma/2$. It is important to note that this relation is specific for σ parallel to the boundary (and for the wave vector of incident light lying in the yz plane).

Consider now the case where σ and the incident light wave vector still lie within the yz plane, but σ is no longer parallel to the boundary, but rather makes an angle γ with the y axis. In this case the Bragg condition takes the form $2k \sin \tilde{\theta}_B = \sigma$, where $\tilde{\theta}_B = \sin^{-1}(\sigma/2k) - \gamma$. It is easy to see that together with the CUS condition $\mathbf{k}' = -\mathbf{k} + \sigma$ this determines the CUS direction $\theta_{CUS} = \tilde{\theta}_B + 2\gamma$, whereas the reflection angle is $\theta_r = \tilde{\theta}_B$. This latter case can be exploited in experiments.

Generalization of our theory to the case of finite γ amounts to the replacement of the functions C and S in Eqs. (16) and (17) for the CUS and CBS by

$$C_{\tilde{\Omega}, \tilde{\phi}} = \cos \tilde{\Omega} z - i \sin \tilde{\phi} \sin \tilde{\Omega} z, \quad (24)$$

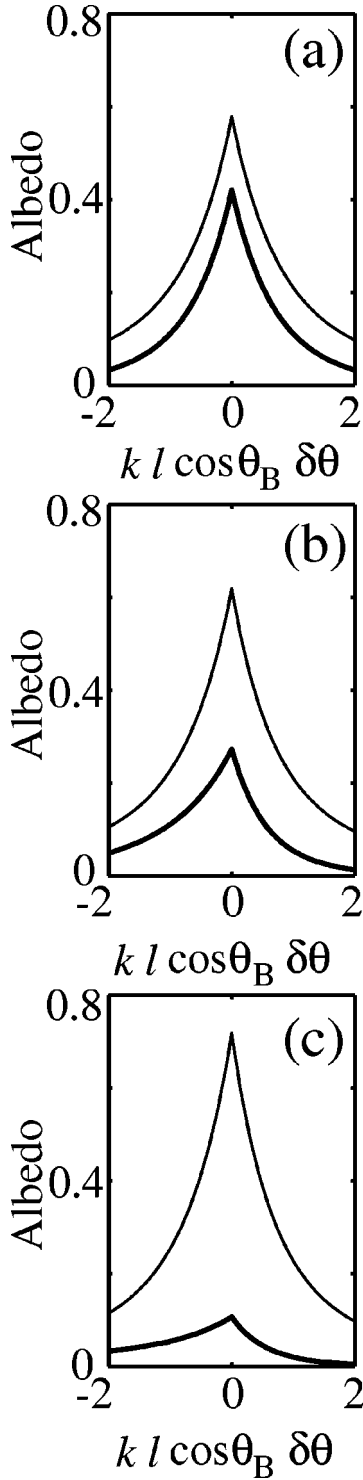


FIG. 3. CBS (thin line) and CUS (bold line) peaks at $L_B = 0.3l$ normalized to the CBS peak height at $L_B/l \rightarrow \infty$ are plotted for detuning (a) $\beta = 0$; (b) $|\beta| = (kl \cos \theta_B)^{-1}$; (c) $|\beta| = 2(kl \cos \theta_B)^{-1}$. The peak maxima occurring at $\delta\theta = \beta$ ($\delta\theta = -\beta$) for the CBS (CUS) are shifted to $\delta\theta = 0$ for convenience.

$$S_{\tilde{\Omega}, \tilde{\phi}} = \left[\frac{\cos \tilde{\theta}_B}{\cos(\tilde{\theta}_B + 2\gamma)} \right]^{1/2} \sin \tilde{\phi} \sin \tilde{\Omega} z, \quad (25)$$

where

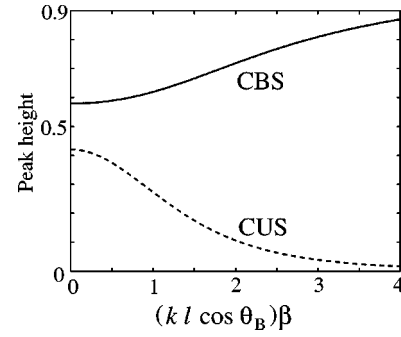


FIG. 4. CBS and CUS peak heights normalized to the CBS peak height at $L_B/l \rightarrow \infty$ plotted vs the detuning $(kl \cos \theta_B)\beta$ at $L_B = 0.3l$.

$$2\tilde{\Omega} = \frac{\sin \theta_B}{\tilde{L}_B \cos(\tilde{\theta}_B + 2\gamma)} \sqrt{(2k\tilde{L}_B \cos(\tilde{\theta}_B + \gamma)\beta)^2 + 1} \quad (26)$$

is the modified splitting between the two solutions of Eq. (9) for k_z . The modified Bragg length in Eq. (26) is defined as $\tilde{L}_B = L_B \sqrt{\cos \tilde{\theta}_B / \cos(\tilde{\theta}_B + 2\gamma)}$. The parameter $\tilde{\phi}$ in Eq. (26) is still given by Eq. (14) with $L_B \rightarrow \tilde{L}_B$.

To derive Eqs. (24)–(26) it is convenient to perform a rotation of the coordinate system by the angle γ . Then the additional factors in Eqs. (25) and (26) as compared to $\gamma = 0$ emerge due to the modification of the boundary conditions. Other steps of the derivation remain unchanged.

It is seen from Eqs. (25) and (26) that the prefactors diverge at $2\gamma = \pi/2 - \tilde{\theta}_B$. This divergence corresponds to the physical situation where the diffracted component of the incident light is aligned with the boundary. With regard to the coherent scattering, the condition $2\gamma = \pi/2 - \tilde{\theta}_B$ manifests a crossover to a new regime. In this regime the diffracted wave does not “fit” into the medium, so that the CUS peak is absent. Formally, for $2\gamma > \pi/2 - \tilde{\theta}_B$ Eq. (9) does not have real solutions for k_z for small β , which corresponds to the opening of the photonic band gap in the z direction. As a result, the CBS peak exhibits an anomaly in the vicinity of the Bragg condition.¹⁶

We did not address in the present work the modifications of the theory caused by a difference of refraction indices on

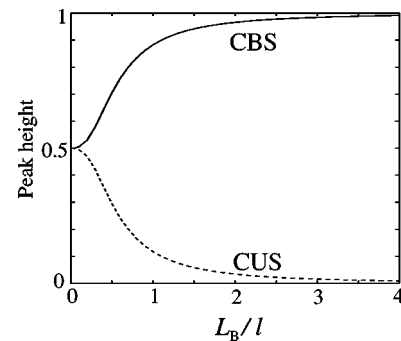


FIG. 5. CBS and CUS peak heights normalized to the CBS peak height at $L_B/l \rightarrow \infty$ plotted vs L_B/l .

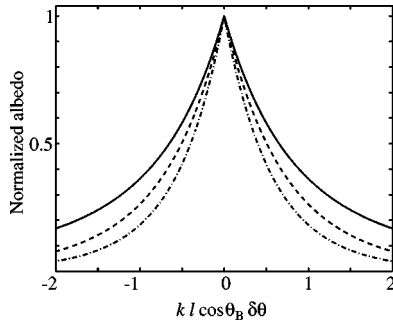


FIG. 6. Normalized CUS albedo at exact resonance, $\beta=0$, shown for $L_B=0.3l$ (dashed line) and $L_B=l$ (dot-dashed line). Solid line: normalized CBS albedo at $\delta\theta=0$ and $L_B=0.3l$.

two sides of the interface. The impact of the light refraction on the CBS was intensively studied (see Ref. 10 and references therein). A nontrivial consequence of the refraction index mismatch is that in the course of diffusion the light wave can ‘‘strike’’ the boundary at an angle exceeding the angle of total internal reflection. Basically, the CUS can be viewed as a mirror image of the CBS, hence the effect of the index mismatch on CUS is similar to that on CBS.

ACKNOWLEDGMENTS

This work was supported in part by the Petroleum Research Fund under ACS-PRF Grant No. 34302-AC6, and the Army Research Office Grant No. DAAD 19-0010406.

APPENDIX

In the vicinity of the Bragg resonance, $k_y \sim \sigma/2$, we employ the coupled wave approach, i.e., we search for the field inside the medium with the dielectric function given by Eq.

(8) in the form of a sum of two waves with wave vectors \mathbf{k} and $\mathbf{k}-\boldsymbol{\sigma}$ and amplitudes $A_{\mathbf{k}}$ and $A_{\mathbf{k}-\boldsymbol{\sigma}}$, respectively. Substitution of this form into the wave equation results in the following system of coupled equations for the wave amplitudes:

$$[(k \cos \theta_B)^2 - k_z^2 - 2k \sin \theta_B (k_y - k \sin \theta_B)]A_{\mathbf{k}} + k^2 \delta\epsilon A_{\mathbf{k}-\boldsymbol{\sigma}} = 0, \quad (\text{A1})$$

$$k^2 \delta\epsilon A_{\mathbf{k}} + [(k \cos \theta_B)^2 - k_z^2 + 2k \sin \theta_B (k_y - k \sin \theta_B)]A_{\mathbf{k}-\boldsymbol{\sigma}} = 0,$$

where we used the definition of the Bragg angle $\sin \theta_B = \sigma/(2k)$. The system (A1) together with the assumption $\cos \theta \approx \cos \theta_B$ lead to Eq. (9).

It is convenient to express the modulation strength $\delta\epsilon$ in terms of the Bragg decay length, L_B , given by

$$L_B = \frac{2 \sin^2 \theta_B}{\sigma \delta\epsilon}. \quad (\text{A2})$$

It is easy to see from Eq. (A2) that the meaning of L_B is the decay length for light of frequency $\omega = kc$ in the middle of the Bragg gap, when the medium boundary is perpendicular to the modulation direction y .

If the condition given in Eq. (9) is satisfied, then there exists a nontrivial solution of the system (A1),

$$\lambda_{1,2} = \frac{A_{\mathbf{k}-\boldsymbol{\sigma}}}{A_{\mathbf{k}}} = \frac{\cos \phi \pm 1}{\sin \phi}, \quad (\text{A3})$$

with ϕ defined by Eq. (14). The two signs in the numerator correspond to the two solutions of Eq. (9) for k_z . Upon matching the solution for the field amplitude with the incident wave, the resulting field can be cast in the form of Eq. (11).

¹M.P. van Albada and A. Lagendijk, Phys. Rev. Lett. **55**, 2692 (1985).

²P.E. Wolf and G. Maret, Phys. Rev. Lett. **55**, 2696 (1985).

³E. Akkermans, P.E. Wolf, and R. Maynard, Phys. Rev. Lett. **56**, 1471 (1986).

⁴S. Etemad, R. Thompson, and M.J. Andrejco, Phys. Rev. Lett. **57**, 575 (1986).

⁵M. Kaveh, M. Rosenbluh, I. Edrei, and I. Freund, Phys. Rev. Lett. **57**, 2049 (1986).

⁶M.P. van Albada, M.B. van der Mark, and A. Lagendijk, Phys. Rev. Lett. **58**, 361 (1987).

⁷S. Etemad, R. Thompson, M.J. Andrejco, S. John, and F.C. MacKintosh, Phys. Rev. Lett. **59**, 1420 (1987).

⁸P.E. Wolf, G. Maret, E. Akkermans, and R. Maynard, J. Phys. (France) **49**, 63 (1988).

⁹*Scattering and Localization of Classical Waves in Random Media*, edited by P. Sheng (World Scientific, Singapore, 1990).

¹⁰M.C.W. van Rosum and T.M. Nieuwenhuizen, Rev. Mod. Phys. **71**, 313 (1999).

¹¹S. John, in *Photonic Band Gaps and Localization*, Vol. 308 of *NATO Advanced Study Institute Series B: Physics*, edited by C. M. Soukoulis (Plenum Press, New York, 1993), p. 1.

¹²J. D. Joannopoulos, R. D. Meade, and J. N. Winn, *Photonic Crystals: Molding the Flow of Light* (Princeton University Press, Princeton, NJ, 1995).

¹³E.E. Gorodnischev, S.L. Dudarev, D.B. Rogozkin, and M.I. Ryzanov, Zh. Eksp. Teor. Fiz. **96**, 1801 (1989) [Sov. Phys. JETP **69**, 1017 (1989)].

¹⁴E. Akkermans, P.E. Wolf, R. Maynard, and G. Maret, J. Phys. (France) **49**, 77 (1988).

¹⁵M.J. Stephen and G. Gwilich, Phys. Rev. B **34**, 7564 (1986).

¹⁶J. Huang, N. Eradat, M.E. Raikh, Z.V. Vardeny, A.A. Zakhidov, and R.H. Baughman, cond-mat/0006175 (unpublished).